Phase behavior and blue-phase-III–isotropic critical point in (*R*)-(*S*) mixtures of a chiral liquid crystal with a direct twist-grain-boundary to blue-phase transition

P. Jamée and G. Pitsi
Laboratorium voor Akoestiek en Thermische Fysica, Katholieke Universiteit Leuven, Celestijnenlaan 200D, 3001 Heverlee, Belgium

M. -H. Li
Laboratoire Physico-Chimie Curie, CNRS/Institut Curie, 11 Rue Pierre et Maríe Curie, 75231 Paris Cedex 05, France

H. -T. Nguyen and G. Sigaud
Centre de Recherche Paul Pascal, CNRS, Université de Bordeaux I, Avenue A. Schweitzer, 33600 Pessac Cedex, France

J. Thoen
Laboratorium voor Akoestiek en Thermische Fysica, Katholieke Universiteit Leuven, Celestijnenlaan 200D, 3001 Heverlee, Belgium
(Received 28 December 1999)

We have investigated mixtures of the (*R*) and (*S*) enantiomers of a chiral liquid crystal, (*R*)- or (*S*)-1-methylheptyl 3′-fluoro-4′-(3-fluoro-4-octadecyloxybenzoyloxy)tolane-4-carboxylate using high-resolution adiabatic scanning calorimetry. The pure (*R*) compound has a direct transition from the twist-grain-boundary to the blue phase without an intermediary chiral nematic phase. For the blue phases a different kind of phase behavior as a function of enantiomeric excess is observed, most probably related to the presence of a twist-grain-boundary-*A* instead of a chiral nematic phase below the blue phases. The general form of this phase diagram is compared with traditional blue-phase behavior. Furthermore a blue-phase-III–isotropic phase critical point, analoguous to that of a liquid-gas system, is observed, consistent with experimental and theoretical work recently published in this field. Finally, the effect of changing enantiomeric excess on the latent heats of the different first order phase transitions is measured and discussed.

PACS number(s): 64.70.Md, 65.20.+w, 61.30.−v

I. INTRODUCTION

The remarkable properties of liquid crystals are related to their symmetry, which is intermediate between the symmetry of liquids and crystals. Over the years a number of theoretical ideas and high-resolution experiments have shaped our understanding of the ''classical'' liquid crystalline nematic (*N*) and smectic (Sm-*A* or Sm-*C*) phases [1,2]. Though it is now well established that (calamitic) chiral liquid crystals can exhibit a number of other phases, such as chiral nematic (*N**), chiral smectic-*C* (Sm-*C**), twist-grain-boundary (TGB), and blue phases (BPs), which a nonchiral compound cannot, it was only about ten years ago that a liquid crystal phase consisting of chiral molecules was predicted theoretically by Renn and Lubensky [3] on the basis of de Gennes' analogy between the liquid crystalline smectic-*A* phase and superconductors [4]. The predicted twist-grain-boundary-*A* (TGBA) phase, which is equivalent to the Abrikosov flux lattice phase of type II superconductors in an external magnetic field, consists of twisting Sm-*A* slabs mediated by grain boundaries of parallel screw dislocations. A chiral version of the *N*–Sm-*A*–Sm-*C* model of Chen and Lubensky [5] (i.e., the model describing the multicritical *NAC* point) was investigated by Lubensky and Renn [6]. A twist-grain-boundary-*C* (TGBC) phase, consisting of smectic-*C* slabs, was subsequently predicted [7,8]. The TGBA and TGBC phases were observed experimentally by Goodby *et al.* [9,10] and Nguyen *et al.* [11], respectively. For a comparison between the experimental phase diagram of chiral systems and the theoretical diagram based on the chiral Chen-Lubensky model, we refer to the recent article of Garland [12].

A second kind of frustrated phase of chiral molecules, the blue phases, results from the competition between the chiral forces and the desire for molecules to pack in ways such that they fill space uniformly. Theoretical and experimental work has demonstrated that cholesteric liquid crystals of short pitch can form up to three distinct blue phases [13–15] between the chiral nematic and isotropic phases. They are named blue phase I (BPI), blue phase II (BPII), and blue phase III (BPIII) in order of ascending temperature. BPI and BPII have, respectively, body-centered cubic and simple cubic symmetry. BPIII is seemingly amorphous with a still unknown local structure. Blue phases are normally found between the isotropic liquid state and a chiral nematic phase of sufficiently short pitch in the sequence *N**-BPs-*I*, except in a few cases where a direct BPI–Sm-*A* transition has been observed [16,17].

However, Li, Nguyen, and Sigaud [18] recently reported the observation of a different phase sequence Sm-*C**–TGBC–TGBA–BPs–*I* in a fluoro-substituted chiral tolane derivative, 1-methylheptyl 3′-fluoro-4′-(3-fluoro-4-octadecyloxybenzoyloxy)tolane-4-carboxylate (abbreviated as FH/FH/HH-18BTMHC), where a direct TGB to BP transition is observed in the absence of an intermediary cholesteric phase. In a recent paper [19] we reported on the results obtained by high-resolution adiabatic scanning calorimetry (ASC) employed to study the phase transitions in the same chiral liquid crystalline material. In this way we were able to determine the heat capacity of the different phases and phase

transitions as well as the enthalpy changes of the material at these transitions.

The ASC method indeed allows for a direct determination of the enthalpy increase at the different phase transitions, and thus is able to disinguish between continuous (second order) and (weakly) first order transitions, and can determine the latent heat of the latter. It is also a high-resolution technique suitable for the determination of details of C_p anomalies at the transitions. The merit of the ASC method has already been extensively proved in our earlier calorimetric investigations on liquid crystals [14,20] and also on the fullerite C_{60} [21].

In this paper we report on the phase behavior as a function of enantiomeric excess of FH/FH/HH-18BTMHC using ASC. Perhaps the most elegant way to examine the influence of chirality is to mix together the (*R*) and (*S*) enantiomers of such a compound in different amounts. In this way, to good approximation only the chirality of the mixture is changed without much effect on other parameters (e.g., due to diastereomeric interactions). Phase diagrams are given and discussed, showing a different kind of phase behavior of the BPs in the presence of a TGBA instead of a N^* phase. The effect of changing enantiomeric excess on the latent heats of the different first order phase transitions is studied. Of particular interest in our study is also the $C_p(T)$ behavior observed on going from the BPIII to the isotropic phase, which is not a real transition in the pure (*R*) compound (at highest chirality) but merely a supercritical C_p increase. We will show that this transition evolves toward a BPIII-*I* critical point and eventually becomes first order by lowering the chirality [i.e., by increasing the (*S*) fraction in the mixture]. This evolution fits in with the experimental and theoretical work recently published in this field [22–24].

II. EXPERIMENT

A. Adiabatic scanning calorimetry

Measurements have been carried out using an adiabatic scanning calorimeter consisting of three stages, the inner stage being the sample enclosed in a holder, surrounded by the second stage, which is a temperature-controlled shield. The whole is submerged in a third, water thermostat stage in order to achieve good thermal stability (fluctuations in the preset temperature difference of 5 K between the thermostat and the second stage can be limited to 15 mK). Temperature differences between the inner and second stages can be kept within ± 0.3 mK during an entire scan. Heating and cooling runs can be carried out at very slow scanning rates, typically of 2 mK/min, ensuring that thermodynamic equilibrium is achieved. When a known constant heating (cooling) power P is applied to the inner stage, the experimental curve of its temperature versus time, $T(t)$, results directly in the enthalpy change,

$$H(T)-H(T_s)=\int_{T_s}^{T_{\rm tr}} C_p dT+\Delta H_L+\int_{T_{\rm tr}}^{T} C_p dT$$
$$=P(t_i-t_s)+P(t_f-t_i)+P(t-t_f), \quad (1)$$

where the index s refers to the starting conditions. When a first order transition occurs, the temperature will remain essentially constant at the transition temperature $T_{\rm tr}$ during a finite time interval $t_f-t_i=\Delta H_L/P$, where ΔH_L is the latent heat. A clear distinction must be made between the actual latent heat ΔH_L (i.e., the enthalpy jump at a first order transition) and pretransitional enthalpy increases, the total transition heat being the sum of both. It must also be noted that, in practice, first order transitions usually have a two-phase coexistence region, due to impurities or inhomogeneities in the sample, so the latent heat jump is broadened over a (small) temperature interval. The heat capacity C_p of the inner stage is the sum of the contributions C_h of the holder and C_s of the sample,

$$C_p=C_s+C_h=\frac{P}{\dot{T}}, \quad (2)$$

where $\dot{T}\equiv dT/dt$ is obtained by numerical differentiation of $T(t)$. By subtracting the holder contribution and dividing by the sample mass the specific heat capacity of the sample is found. Sufficiently large quantities of sample have to be used to make C_s large enough compared to C_h, in order to obtain good results on the specific heat capacity. Consecutive mixtures were prepared by adding pure (*R*) or (*S*) enantiomer to the previous mixture in the cell in order to limit the total amount of material used. Further details concerning the ASC calorimetric technique can be found elsewhere [25].

B. Compounds

The compound we have investigated is a chiral fluorosubstituted tolane derivative, (*R*)- or (*S*)-FH/FH/HH-18BTMHC:

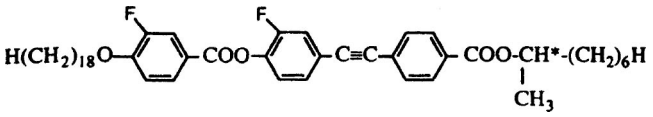

This compound was synthesized and characterized by Li, Nguyen, and Sigaud [18], and further investigated using polarization microscopy, differential scanning calorimetry (DSC), helical pitch measurements, x-ray structural analysis, and electro-optical studies [26]. In this compound, a direct TGB to BP transition, without an intermediary N^* phase, was experimentally observed. The full phase sequence is Sm-*C**–TGBC–TGBA–BPI–BPII–BPIII–*I*. A new batch of the (*R*) and (*S*) enantiomer was especially synthesized for further investigation with an ASC calorimeter. While DSC measurements on the pure (*R*) compound found BPI only on cooling, high-resolution ASC scans revealed the presence of BPI also on heating [19]. It was found that all transitions in the pure (*R*) compound were first order, with the exception of BPIII-*I*, which does not represent a real phase transition, but is merely a supercritical $C_p(T)$ anomaly. A further ASC investigation as a function of enantiomeric excess of phase behavior and phase transitions, latent heats of the first order transitions, and the evolution of the BPIII-*I* supercritical feature is described in this work.

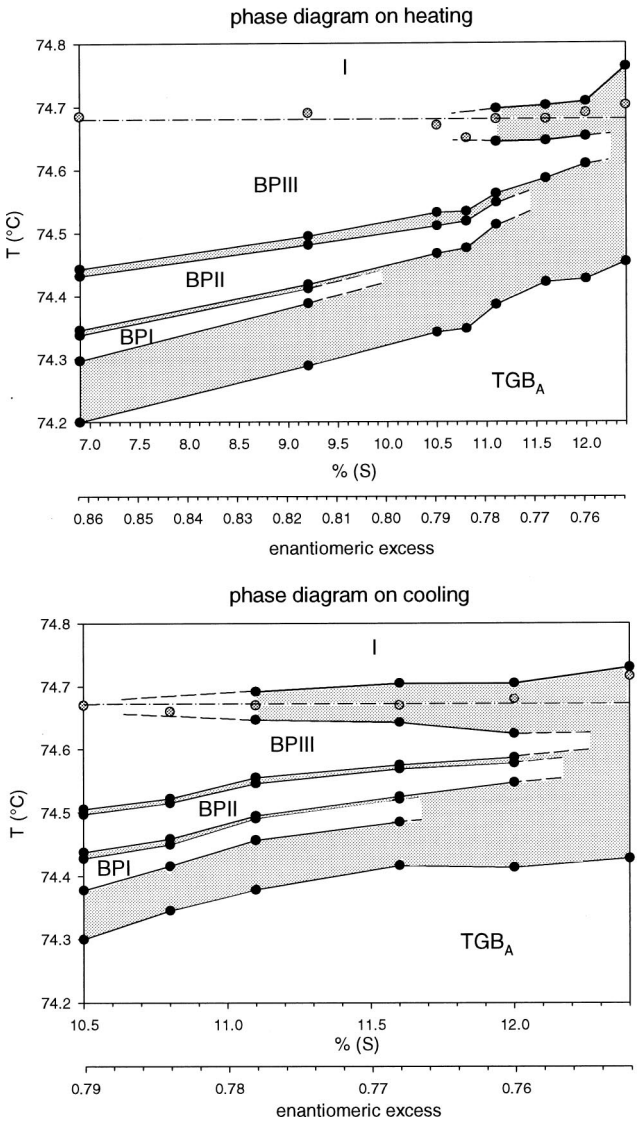

FIG. 1. Detail of the phase diagram in the TGBA-BPs-*I* temperature region on heating and on cooling. Data at low (*S*) concentrations are omitted for clarity. Full dots represent beginning or end of the two-phase regions of the transitions. Temperatures of maxima in the BPIII-*I* C_p peak are indicated by gray dots. Lines were added as guides for the eyes. Solid lines connect the data points and dashed lines extrapolate phase behavior between investigated concentrations. The dash-dotted line connects the BPIII-*I* peak temperatures. The phase sequence at each concentration can thus be determined from the shape of this diagram.

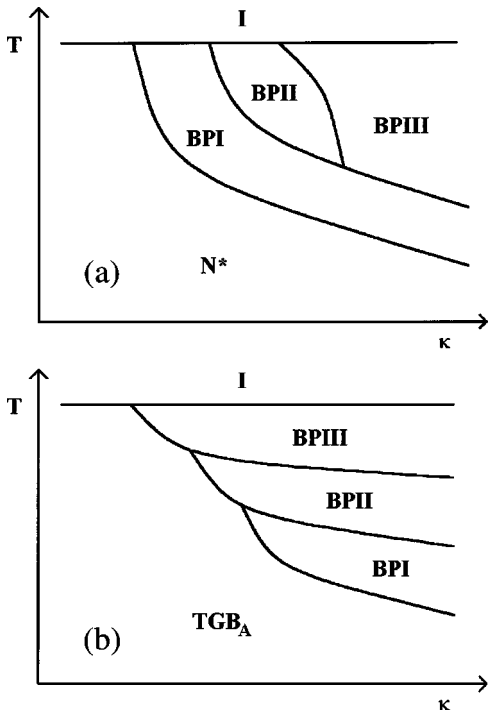

FIG. 2. General form of the temperature (*T*) versus chirality (κ) phase diagram involving blue phases (a) as found in literature with a N^* phase present and (b) as obtained from our experiments with the N^* phase replaced by a TGBA phase.

III. RESULTS AND DISCUSSION

A. TGBA-BPs-*I* region

Enthalpy data show that all TGBA to BP and BP to BP transitions are clearly first order. For simplicity, we will indicate the different mixtures by the molar fraction of the (*S*) enantiomer. In contrast to the traditional representation of a phase diagram, where only transition temperatures are shown, in Fig. 1 we have plotted the beginning and end of the two-phase coexistence regions at the various transitions. This provides a much clearer insight into the phase behavior with changing enantiomeric excess. For reasons of clarity, the (*S*) fractions below 6.9% on heating and 10.5% on cooling are not shown. Simply by looking at the shape of the diagram presented in this way, one can derive the phase sequence at different (*S*) fractions. It must be noted that calorimetric data cannot determine the nature of the phases present in a compound. However, the initial identification of the phases was performed by Li *et al.* [18] for the pure (*R*) compound. No change in the number of phases occurred between the pure compound and the 6.9% mixture on heating and the 10.5% mixture on cooling so it is clear that the same phase sequence Sm-C^*–TGBC–TGBA–BPI–BPII–BPIII–*I* is present in the aforementioned mixtures. While the general shape of the phase diagram seems to be the same on heating and on cooling there is a difference in the (*S*) fractions where the BPs disappear. In both cases, BPI vanishes at the lowest (*S*) fraction, on heating between 9.0% and 10.5% (*S*) and on cooling between 11.6% and 12.0% (*S*), leaving a TGBA-BPII transition at higher (*S*) fractions. On heating, BPII vanishes between 11.1% and 11.6%, leaving a TGBA-BPIII transition. Between 12.0% and 12.4% the third blue phase BPIII disappears, so only a direct TGBA to isotropic phase transition remains. On cooling, however, both BPII and BPIII persist until 12.0% but they are no longer present at 12.4%, where also only a direct TGBA-*I* phase transition remains. It does not seem unreasonable to assume that on cooling the BPs vanish in the same order as on heating, i.e., with increasing (*S*) fraction first BPI, then BPII, and finally BPIII. The general shape of the phase diagram thus derived from our data is quite different from what is known in the literature [22,27] (see Fig. 2). The fact is that in the ''traditional'' case a chiral nematic phase is present on the low-temperature side of the BPs, while in our case a TGBA phase seems to influence the phase behavior of the BPs above it. This is the first time that such phase behavior has been ob-

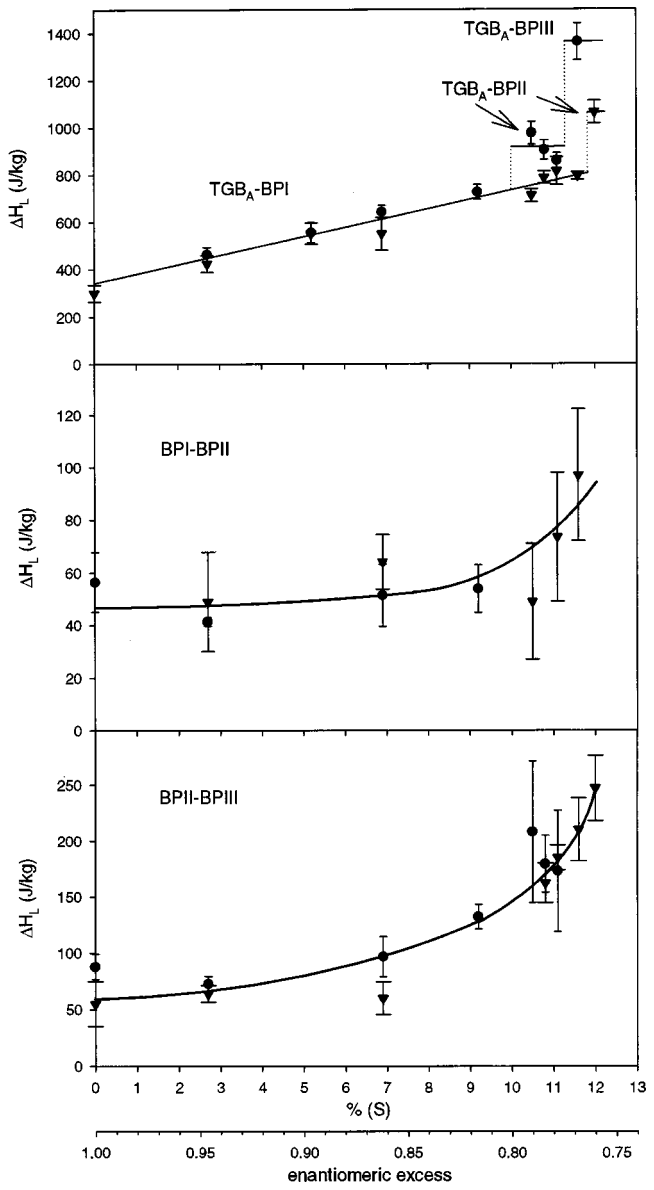

FIG. 3. Latent heats of the TGBA to blue phase and blue phase to blue phase transitions as a function of (*S*) concentration and enantiomeric excess, on heating (dots) and on cooling (triangles). All lines are guides for the eye. Note that certain transitions exist only in a limited concentration interval.

served to our knowledge and a theoretical investigation into this phenomenon would be useful.

The evolution of the latent heats with changing enantiomeric excess is plotted in Fig. 3. The BPII-BPIII latent heat shows an increase with increasing (*S*) fraction (i.e., with decreasing enantiomeric excess). The small BPI-BPII latent heats (typically 50 J/kg) show a slight increase at higher (*S*) fractions. The TGBA-BPI latent heat shows a roughly linear increase with increasing (*S*) fraction. Between 9.2% and 10.5% (*S*), BPI vanishes on heating, and the latent heat of the remaining TGBA-BPII transition is significantly larger than that of the TGBA-BPI transition. It seems that this latent heat is roughly equal to the combined TGBA-BPI and BPI-BPII transition heats. On cooling, the phase sequence remains the same and the linear increase persists until 11.6% (*S*), where BPI vanishes on cooling. There we see a similar increase in

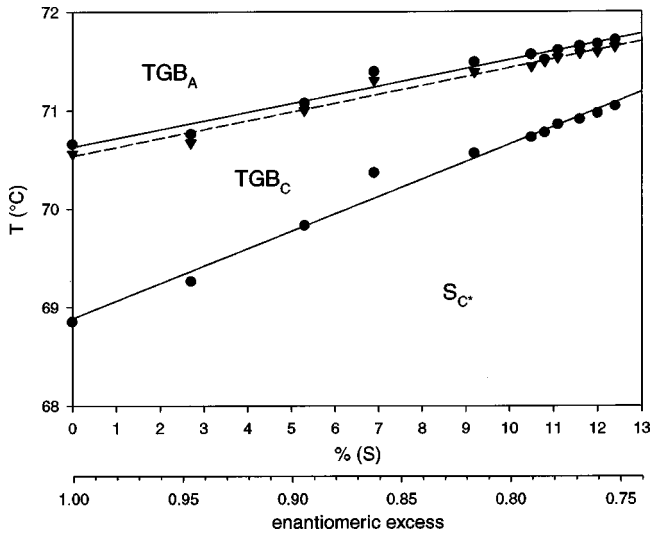

FIG. 4. Phase diagram in the Sm-*C**–TGBA–TGBC temperature region. These transitions are very sharp, so we have plotted only the temperatures of the maxima of the C_p peaks on heating (dots) and on cooling (triangles), as in a traditional phase diagram. In the temperature region studied the Sm-*C** phase is observed only on heating due to supercooling of the TGBC phase on cooling. Lines represent linear fits through the data points. Solid lines: on heating; dashed line: on cooling. Notice the clear thermal hysteresis of the TGBA-TGBC transition due to its first order character.

the latent heat of the TGBA-BPII transition compared to the TGBA-BPI values. However, this increase is slightly larger than that on heating. This is in agreement with the fact that the BPI-BPII latent heat on cooling at 11.6% (*S*) is slightly larger than that on heating at 9.2% (*S*), and again the TGBA-BPII latent heat is roughly equal to the sum of the TGBA-BPI and BPI-BPII transition heats. On heating, a second sudden increase in the latent heat is observed where BPII vanishes between 11.1% and 11.6% (*S*). This increase is much larger than the first increase on heating, but this can be related to the fact that the BPII-BPIII latent heat is much larger than that of BPI-BPII. So again we see that the latent heat of the remaining TGBA-BPIII transition is roughly equal to the sum of the TGBA-BPII and BPII-BPIII transition heats.

B. Sm-*C**–TGBC–TGBA region

From the phase diagram in the Sm-*C**–TGBC–TGBA temperature region studied (Fig. 4), we notice that the Sm-*C** phase is observed only on heating. This is caused by a supercooling of the TGBC phase on cooling, as was already observed by Li *et al.* [18]. The Sm-*C**–TGBC and TGBC-TGBA transitions are first order. From Fig. 5 we can see that the latent heat of the Sm-*C**–TGBC transition remains constant at approximately 35 J/kg, while the TGBA-TGBC latent heat shows a decreasing trend from about 80 in the pure (*R*) compound to about 40 J/kg at the highest investigated (*S*) fraction. Also, the two-phase regions of these transitions were quite small (typically 50 mK), so in this case we have plotted only the peak temperatures (i.e., the temperatures of the maxima in the C_p peaks at the transitions) in the phase diagram (Fig. 4). One can observe a roughly linear increase in the transition temperature for both transitions: the

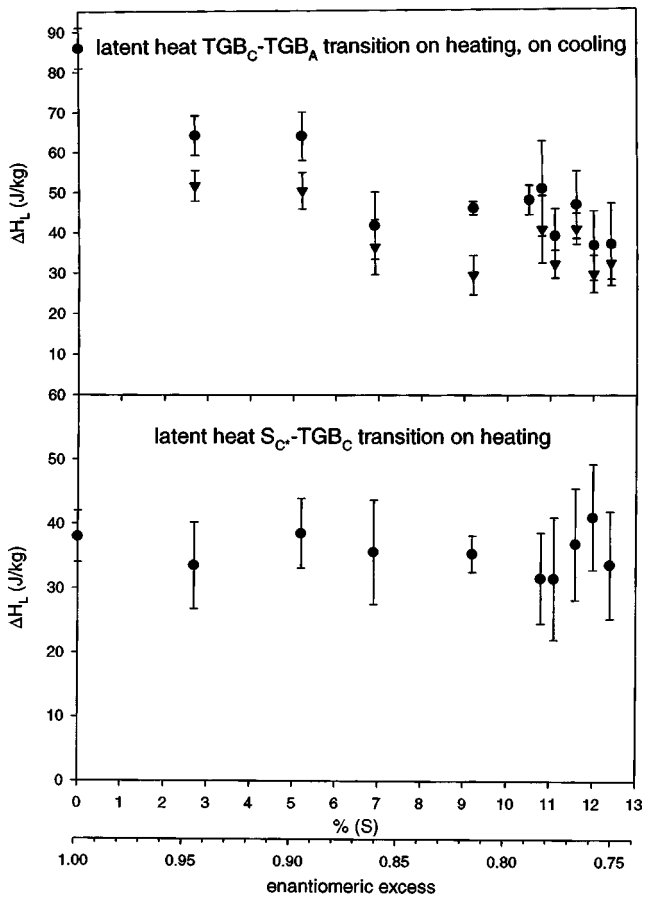

FIG. 5. Latent heats of the Sm-C^*–TGBC and TGBC-TGBA transitions as a function of (*S*) concentration and enantiomeric excess on heating (dots) and on cooling (triangles).

lines in Fig. 4 are linear fits through the transition temperatures. A clear thermal hysteresis is present at the TGBC-TGBA transition, confirming its first order character. This is, however, in contradiction with the mean-field Lubensky-Renn chiral version [6] of the Chen-Lubensky multicritical *NAC* model [5] predicting a continuous TGBC-TGBA transition [7,8,12]. One also notices a decrease of the TGBC temperature region with increasing (*S*) fraction, indicating that this phase will probably vanish at lower enantiomeric excess (i.e., at lower chirality) as can be expected from the Renn-Lubensky model. This decrease is accompanied by the decreasing trend of the TGBA-TGBC latent heat in Fig. 5.

C. BPIII-*I* evolution and critical point

Over the last few years, much attention has been given to the BPIII-*I* transition. In the chiral liquid crystals CE4 and CE6, ASC experiments have shown the presence of a finite BPIII-*I* latent heat [28] and a discontinuous jump in rotary power and scattered light intensity has been observed [29], proving this transition to be first order. However, investigations in the highly chiral liquid crystal *S*,*S*-MHBBC (often denominated as CE2) show no evidence of a first order transition [30]. This has led to the assumption that, much as in a liquid-gas system, there exists a first order coexistence line terminating in a BPIII-*I* critical point (CP). A theoretical approach to the explanation of such a behavior is provided by Lubensky and Stark [22]. Further investigation of mixtures of *S*,*S*-MHBBPC and its racemic by Kutjnak *et al.* [23] have experimentally confirmed the existence of a BPIII-*I* critical point. Recently, Anisimov, Ayagan, and Collings [24] have formulated an analogy between the BPIII-*I* and the liquid-gas critical points in order to clarify the pre-

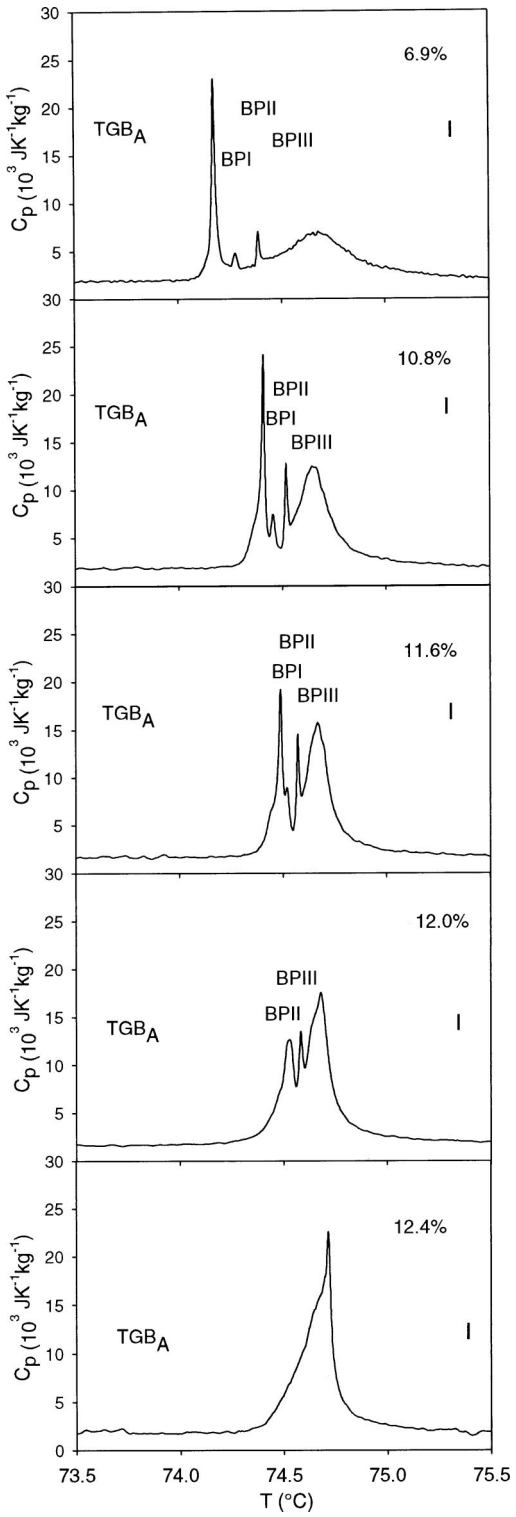

FIG. 6. Evolution of the specific heat capacity in the TGBA-BPs-*I* region with increasing (*S*) concentration, on cooling. A supercritical BPIII-*I* C_p anomaly at low (*S*) concentrations evolves to a first order transition at higher (*S*) concentrations through a critical point, located between 10.5% and 11.1% (*S*).

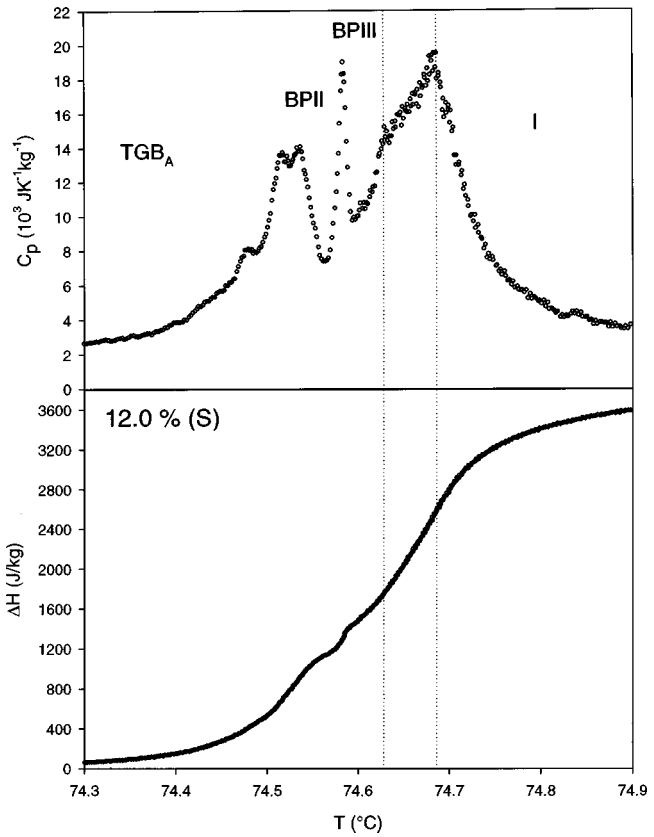

FIG. 7. Detail of the TGBA-BPII-BPIII-*I* transitions for an (*S*) fraction of 12.0% on cooling. The BPIII-*I* peak shows a characteristic flattening of the top, indicating the presence of a two-phase coexistence region at a first order transition (width indicated by dotted lines). This coincides with the latent heat observed in the enthalpy in this temperature region. A baseline has been subtracted from the enthalpy curve for reasons of clarity.

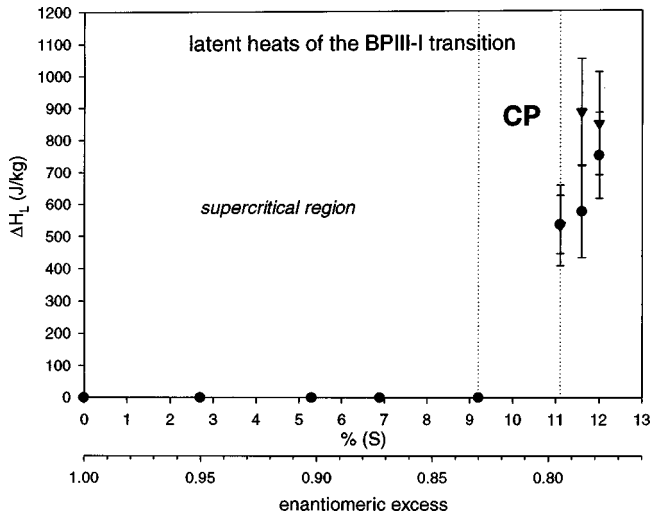

FIG. 8. Latent heats of the BPIII-*I* transitions on heating (dots) and on cooling (triangles). The location of the BPIII-*I* critical point (CP) is expected between 9.2% and 11.1% (*S*) (indicated by dotted lines). The supercritical region is also indicated.

transitional behavior of physical properties in the vicinity of such a CP. This theory is indeed in good agreement with the heat capacity data of [23].

The evolution of the BPIII-*I* $C_p(T)$ peak in FH/FH/HH-18BTMHC with changing enantiomeric excess (on cooling) is illustrated in Fig. 6. It shows a clear evolution from a broad, supercritical to an increasingly sharper and steeper peak. We attribute this to the evolution of a supercritical $C_p(T)$ anomaly, through a BPIII-*I* critical point, to a first order transition.

A close investigation of the BPIII to isotropic transition heat capacity and enthalpy data reveals that the CP is located in the vicinity of an (*S*) fraction of 10.5%. At (*S*) fraction of 11.1% and higher, evidence for the presence of a finite latent heat was found. This includes a characteristic ''flattening'' of the heat capacity peaks, indicating a two-phase coexistence region, and thus a first order transition, as is illustrated in Fig. 7. A small thermal hysteresis could be observed as well. Values obtained for the width of the two-phase regions are around 50 mK, meaning that the first order BPIII-*I* transitions are fairly broad which makes the determination of their latent heat less precise. Values for the BPIII-*I* latent heats are given in Fig. 8. They show an increasing trend with increasing (*S*) fraction. At the investigated (*S*) fractions of 9.2% and below, no such evidence supporting the presence of a latent heat was observed. Measurements in between do not show convincing evidence for either case. This places the CP between 9.2% and 11.1% (*S*), as is also indicated in Fig. 8.

A more quantitative approach to the determination of the location of the CP could possibly be achieved through the model developed by Anisimov *et al.* [24], which provides an expression for the $C_p(T)$ curve near a BPIII-*I* critical point with five independent parameters, which could be obtained by fitting our results. One of these fit parameters is proportional to the difference $X-X_c$ between the (*S*) fraction X and the critical fraction X_c from which the latter can be determined. Future work will consist of an attempt to use this method to corroborate the location of the CP. However, the superposition of first order TGBA-BP and BP-BP transitions on the BPIII-*I* peak will prevent the application of this model on the low-temperature side of this peak, and this is likely to make the determination of X_c in this fashion less reliable or even impossible.

IV. CONCLUSIONS

A high-resolution ASC investigation was carried out on mixtures of the (*R*) and (*S*) enantiomers of a fluorosubstituted tolane derivative, abbreviated as FH/FH/HH-18BTMHC, between (*S*) fractions of 0.0 and 12.4%. This compound has a phase sequence Sm-*C**–TGBC–TGBA–BPI–BPII–BPIII–*I*, that is, a direct TGB to BP transition without an intermediary *N** phase.

The ASC technique not only is able to perform high-resolution heat capacity measurements, but can also perform a direct measurement of the enthalpy change as a function of temperature. From the former, latent heats of (weakly) first order transitions can be obtained.

It was found that all phase transitions, with the exception of BPIII to isotropic, were clearly first order. We were able to extract the phase behavior in the TGBA-BPs-*I* temperature region from a phase diagram obtained by ASC where the two-phase coexistence regions of the (first order) transi-

tions were plotted. An unusual kind of phase behavior as a function of enantiomeric excess was observed. This is most probably related to the fact that a TGBA phase is present on the low-temperature side of the BPs, instead of a N^* phase as is usually the case. A comparison of the general form of the phase diagram in both cases was made. A theoretical investigation into the origins of this behavior would be useful but is not as yet available.

The changes in the latent heats of the various transitions with changing enantiomeric excess were measured and discussed. It was observed that, upon the vanishing of one of the BPs, the latent heat of the remaining TGBA-BP transition consists of the sum of the transition heats of the previously [i.e., at lower (*S*) fraction] present TGBA to BP and BP to BP transitions.

The BPIII to isotropic transition peak shows a clear evolution from a broad supercritical $C_p(T)$ increase at lower (*S*) fractions to a sharp first order transition at the highest investigated (*S*) fractions. This is attributed to the presence of a BPIII-*I* critical point, analoguous to that of a liquid-gas system, as has been described theoretically [22] and also experimentally in another system [23]. This critical point is located in the vicinity of 10.5% (S), since at (*S*) fractions above 11.1% a latent heat is present, while at (*S*) fractions of 9.2% or below no evidence of such an enthalpy jump was found. Future work on this data will include an analysis of the specific heat capacity data near the BPIII to isotropic critical point using the model proposed by Anisimov *et al.* [24]. It is unlikely, however, that more exact information about the location of the critical point can be obtained using this method, due to the superposition of the first order TGBA-BP and BP-BP transitions on the BPIII-*I* peak.

The phase behavior in the Sm-*C**–TGBC–TGBA temperature region is also given. The Sm-*C**–TGBC and TGBC-TGBA transitions are first order, in contradiction to the Lubensky-Renn model [6–8]. The evolution of their latent heats as a function of enantiomeric excess was investigated.

ACKNOWLEDGMENT

This work was supported by the Fund for Scientific Research Flanders (Belgium) (FWO, Project No. G.0264.97N).

[1] G. Vertogen and W. H. de Jeu, *Thermotropic Liquid Crystals* (Springer-Verlag, Berlin, 1988).
[2] P. G. de Gennes and J. Prost, *The Physics of Liquid Crystals* (Clarendon, Oxford, 1994).
[3] S. R. Renn and T. C. Lubensky, Phys. Rev. A **38**, 2132 (1988).
[4] P. G. De Gennes, Solid State Commun. **10**, 753 (1972).
[5] J.-C. Chen and T. C. Lubensky, Phys. Rev. A **14**, 1202 (1976).
[6] T. C. Lubensky and S. R. Renn, Phys. Rev. A **41**, 4392 (1990).
[7] S. R. Renn and T. C. Lubensky, Mol. Cryst. Liq. Cryst. **209**, 349 (1991).
[8] S. R. Renn, Phys. Rev. A **45**, 349 (1992).
[9] J. W. Goodby, M. A. Waugh, S. M. Stein, E. Chin, R. Pindak, and J. S. Patel, Nature (London) **337**, 449 (1989).
[10] J. W. Goodby, M. A. Waugh, S. M. Stein, E. Chin, R. Pindak, and J. S. Patel, J. Am. Chem. Soc. **111**, 8119 (1989).
[11] H. T. Nguyen, A. Bouchta, L. Navailles, P. Barois, N. Isaert, R. J. Twieg, A. Maroufi, and C. Destrade, J. Phys. II **2**, 1889 (1992).
[12] C. W. Garland, Liq. Cryst. **26**, 669 (1999).
[13] H. Stegemeyer, T. H. Blümel, K. Hiltrop, H. Onusseit, and F. Porsch, Liq. Cryst. **1**, 3 (1986).
[14] J. Thoen, Phys. Rev. A **37**, 1754 (1988).
[15] P. P. Crooker, Liq. Cryst. **5**, 751 (1989).
[16] H. Onusseit and J. Stegemeier, Z. Naturforsch. Teil A **392**, 658 (1984).
[17] H.-T. Nguyen, C. Sallen, A. Babeau, J. M. Galvan, and C. Destrade, Mol. Cryst. Liq. Cryst. **154**, 147 (1987).
[18] M.-H. Li, H.-T. Nguyen, and G. Sigaud, Liq. Cryst. **20**, 361 (1996).
[19] M. Young, G. Pitsi, M.-H. Li, H.-T. Nguyen, P. Jamée, G. Sigaud, and J. Thoen, Liq. Cryst. **25**, 387 (1998).
[20] J. Thoen, H. Marijnissen, and W. Van Dael, Phys. Rev. A **26**, 2886 (1982); Phys. Rev. Lett. **52**, 204 (1984); H. Marijnissen, J. Thoen, and W. Van Dael, Mol. Cryst. Liq. Cryst. **124**, 195 (1985).
[21] G. Pitsi, J. Caerels, and J. Thoen, Phys. Rev. B **55**, 915 (1997).
[22] T. C. Lubensky and H. Stark, Phys. Rev. E **53**, 714 (1996).
[23] Z. Kutnjak, C. W. Garland, C. G. Schwartz, P. J. Collings, C. J. Booth, and J. W. Goodby, Phys. Rev. E **53**, 4955 (1996).
[24] M. A. Anisimov, V. A. Ayagan, and P. J. Collings, Phys. Rev. E **57**, 582 (1998).
[25] J. Thoen, E. Bloemen, H. Marynissen, and W. Van Dael, in *Proceedings of the 8th Symposium Thermophys. Prop. National Bureau of Standards, Maryland, 1981*, edited by J. V. Sengers (American Society of Mechanical Engineers, New York, 1982); J. Thoen, in *Phase Transitions in Liquid Crystals*, edited by S. Martelucci and A. N. Chester (Plenum, New York, 1992), Chap. 10.
[26] M.-H. Li, V. Laux, H.-T. Nguyen, G. Sigaud, P. Barois, and N. Isaert, Liq. Cryst. **23**, 389 (1997).
[27] D. K. Yang and P. P. Crooker, Phys. Rev. A **35**, 4419 (1987).
[28] G. Voets and W. Van Dael, Liq. Cryst. **14**, 617 (1993).
[29] J. B. Becker and P. J. Collings, Mol. Cryst. Liq. Cryst. Sci. Technol., Sect. A **265**, 163 (1995).
[30] Z. Kutnjak, C. W. Garland, J. L. Passmore, and P. J. Collings, Phys. Rev. Lett. **74**, 4859 (1995).